Best Practice for Evaluating Electrocatalysts for the Hydrogen Economy

Matthew A. Bird, Sean E. Goodwin, and Darren A. Walsh*

Nottingham Applied Materials and Interfaces Group

GSK Carbon Neutral Laboratory for Sustainable Chemistry, University of Nottingham, Jubilee Campus, Nottingham NG7 2TU, UK

e-mail: darren.walsh@nottingham.ac.uk

ABSTRACT

Screening new electrocatalysts is key to the development of new materials for next-generation energy devices such as fuel cells and electrolysers. The counter electrodes used in such tests are often made from materials such as Pt and Au, which can dissolve during testing and deposit onto test electrocatalysts, resulting in inaccurate results. The most common strategy for preventing this effect is to separate the counter electrode from the test material using an ion-transporting Nafion membrane. Here, we use X-ray photoelectron spectroscopy, energy-dispersive X-ray analysis, mass spectrometry, and voltammetry to demonstrate the limitations of this approach during constant-current, extended stability testing of electrocatalysts for H_2 evolution. We show that Nafion membranes cannot prevent contamination of carbon electrocatalysts by Pt and Au counter electrodes, leading to an apparent increase in electrocatalytic activity of the carbon. We then demonstrate that carbon counter electrodes in undivided cells can contaminate and deactivate Pt and Au electrocatalysts for H_2 evolution. We show that use of a setup comprising a glass frit separating a carbon counter electrode from the test electrocatalyst can prevent these effects. Finally, we discuss these phenomena using H_2 evolution at MoS_2 and at a $K_6[P_2W_{18}O_{62}](H_2O)_{14}$/carbon nanotube composite as test reactions.

Keywords: Electrocatalysis; water splitting; counter electrode; Nafion; rotating-disk electrode; hydrogen-evolution reaction

INTRODUCTION

The development of earth-abundant electrocatalysts is a key driver in the development of next-generation hydrogen fuel cells and water electrolysers – devices that are expected to play key roles in the emerging hydrogen economy. The development of such systems requires that methods for accurately measuring the activity of electrocatalysts are available, and the method-of-choice is rotating-disk electrode voltammetry.[1-9] Glassy carbon (GC) is usually used as the substrate for electrocatalyst testing, due to its wide electrochemical window and low electrocatalytic activity towards reactions such as the oxygen-evolution reaction (OER), oxygen-reduction reaction (ORR), hydrogen-evolution reaction (HER), and hydrogen-oxidation reaction (HOR).[6,10,11]

Counter electrodes in electrochemical cells are usually fabricated from materials such as Pt and Au, due to their perceived electrochemical inertness.[12] Indeed, Pt has been recommended as a counter-electrode material in guides to electrochemistry and electrocatalysis.[2,9,13] However, if the potential of the counter electrodes becomes sufficiently high during analysis, dissolution of the metal can occur.[14] This effect is exacerbated when the potential of the test electrocatalyst is cycled – a common method for pre-activating electrocatalysts[2] and examining their long-term stability.[3,8,15] For example, if the potential of a Pt electrode is cycled between those at which the ORR and OER occur, repeated reduction of electrogenerated Pt—O species exposes readily-solubilized, low-coordinate Pt.[12,14,16-20] Dissolved Pt ions can reach and become deposited on the electrocatalyst surface, increasing the apparent activity of the test material.[3,7,8,12,21-26] Increasing the surface area of the counter electrode decreases the current density it experiences, and while this can slow the dissolution process, it cannot stop it.[27] Dissolved Cl^- ions (either from the supporting electrolyte or leaking from a reference electrode) can also increase the rate of dissolution of Pt and Au electrodes through the formation of metal-chloride complexes.[12,25]

One of the most common strategies for mitigating the effects of dissolution of Pt counter electrodes is to separate the test electrocatalyst from the counter electrode using a Nafion membrane.[12,22,27-29] However, a search of the literature does not reveal strong evidence for the effectiveness of this strategy. There is, on the other hand, evidence that Nafion is permeable to dissolved Pt ions. For example, Pt ions

dissolving from fuel-cell cathodes can enter and deposit in Nafion proton-exchange membranes during operation.[30-33] Transport of dissolved Pt ions through Nafion membranes has even been used to fabricate membrane-electrode assemblies.[34] Perhaps the most obvious solution to the problem of counter-electrode dissolution is to use non-metal counter electrodes, such as graphite rods.[3-5,7,8,11,24,35,36] Some work has probed the effectiveness of this strategy but, as with earlier studies on Pt dissolution, it was probed using extended potential-cycling tests.[8,24] Real devices would not experience the kind of potential excursions used in accelerated-stability tests and are expected to operate at or near constant currents or potentials. Consequently, testing the long-term stability of electrocatalysts at constant currents is also important.[5]

In this contribution, we first show that Pt counter electrodes contaminate and activate GC electrocatalysts during constant-current HER in undivided cells containing acidic electrolytes. After 24 h, the electrocatalytic activity of the contaminated GC increases such that it is similar to that of pure Pt. We then show that use of a Nafion membrane to separate Pt and Au counter electrodes from the GC is ineffective; microscopic and spectroscopic analysis shows that GC surfaces become covered with Pt and Au after 24 h of HER electrolysis. Electrochemical analysis shows that the use of carbon counter electrodes in undivided cells can lead to the opposite problem; deposition of particulate carbon onto Pt and Au electrocatalysts reduces their electrocatalytic activity for the HER. We show that these problems can be avoided by using a carbon counter electrode separated from the test electrocatalyst by a glass frit. We discuss this strategy using HER at a $K_6[P_2W_{18}O_{62}](H_2O)_{14}$/single-walled carbon nanotube ($K_6[P_2W_{18}O_{62}](H_2O)_{14}$@SWNT) composite and a MoS_2 electrocatalyst as test reactions.

EXPERIMENTAL

Materials and Apparatus. Polishable 5-mm diameter GC, Pt, and Au rotating disk electrodes (Pine Research, Durham, NC) were used as HER electrocatalysts, allowing us to reproduce surfaces with consistent electrocatalytic activity. Pt- and Au-coil counter electrodes were from CH Instruments (Austin, TX) and graphite and glassy-carbon rods were from Alfa Aesar. Ag/AgCl reference electrodes containing

saturated KCl were from CH Instruments and Nafion-117 was from Alfa Aesar. Unless otherwise indicated, 1.0 mol dm^{-3} H_2SO_4 was used as the electrolyte. 100 mg dm^{-3} Pt and Au in 2% HCl standard solutions were from Fischer Scientific. MoS_2 was from Alfa Aesar and was used as received.

Electrochemical testing was carried out using a Model CHI760C potentiostat (CH Instruments) coupled with a modulated speed rotator from Pine Research. X-ray photoelectron spectroscopy (XPS) was carried out using a Kratos AXIS DLD instrument equipped with an Al K_α X-ray source (1486.6 eV). CasaXPS software was used with Kratos sensitivity factors to determine atomic concentrations. A Shirley background correction was applied to all spectra prior to analysis. All spectra were charge corrected to the adventitious carbon peak at 284.8 eV. Fitting of spectral components used the asymmetrical line shapes LF(0.5,1,400,500) and DS(0.01,250) for Pt and Au, respectively. A Zeiss EVO MA10 scanning electron microscope equipped with secondary- and backscattered-electron detectors and an energy dispersive X-ray (Element, AMETEK) analyser was used for scanning electron microscopy (SEM) and elemental detection. The accelerating voltage was 20 kV.

Diluted aliquots of the electrolyte were analysed for Pt and Au by inductively-coupled plasma mass spectrometry (ICP-MS) using an iCAP-Q from Thermo Fisher Scientific (Bremen, Germany) with a collision cell charged with He. Kinetic energy discrimination (KED) was used to remove polyatomic interferences. Samples were introduced at 1.2 cm^3 min^{-1} from an autosampler (Cetac ASX-520) incorporating an ASXpress™ rapid uptake module through a perfluoroalkoxy (PFA) Microflow PFA-ST nebuliser (Thermo Fisher Scientific, Bremen, Germany).

Experimental Methods. GC electrodes were prepared by briefly immersing them in aqua regia, rinsing in milli-Q water, and polishing to a mirror finish with alumina (1.0, 0.3, 0.05 μm, Buehler, Coventry, UK). Pt and Au electrodes were polished to mirror finishes using alumina (1.0, 0.3, 0.05 μm). Prior to use, Pt counter electrodes were flame treated and Au electrodes were rinsed with milli-Q water. Graphite rods were polished with 0.05 μm alumina, rinsed with water, immersed in 1.0 mol dm^{-3} HNO_3 for at least 60 min, then agitated ultrasonically in water. A 3-necked flask, a separable H-cell, or an H-cell containing a built-in glass frit was used for electrochemical measurements. In divided cells, one

compartment contained the test electrocatalyst and the other contained the Ag/AgCl reference electrode and counter electrode. Membranes were immersed in 1.0 mol dm^{-3} H_2SO_4 for at least 20 min before use. Each half of the H-cells contained 20 cm^3 of electrolyte, and approximately 3.14 cm^2 of the counter electrodes were submerged in the electrolyte. The electrolyte was purged with N_2 prior to use, and an N_2 atmosphere was maintained through use of an Atmos bag.

MoS_2 electrodes were fabricated by dispersing MoS_2 in isopropyl alcohol and agitating the dispersion ultrasonically for 30 min. 0.010 cm^3 of the dispersion was drop-cast onto a 5-mm diameter GC electrode to give an approximate loading of 1.8 mg cm^{-2}. The $K_6[P_2W_{18}O_{62}](H_2O)_{14}$@SWNT electrode was prepared by mixing a solution containing 1 wt.% $K_6[P_2W_{18}O_{62}](H_2O)_{14}$@SWNT and 3 wt.% PTFE binder ultrasonically for 20 min. 0.080 cm^3 of the mixture was deposited onto a 3-mm diameter GC electrode surface and allowed to dry in air. Electrochemical testing of this electrocatalyst was carried out using 1.0 mol dm^{-3} HCl purged with Ar as electrolyte, and a saturated calomel reference (SCE) electrode. Unless otherwise indicated, all potentials are reported on the reversible hydrogen electrode (RHE) scale. Constant-current stability tests were carried out by passing −10 mA cm^{-2} through electrocatalysts for 24 h while the electrodes rotated at 1600 rpm.

RESULTS AND DISCUSSION

Contamination of Working Electrodes in Undivided Cells. Our starting point was to examine the effects of driving the HER at GC electrocatalysts in undivided cells. −10 mA cm^{-2} was passed through an undivided cell containing either a Pt or Au counter electrode, an Ag/AgCl reference electrode, and a GC electrocatalyst. Figures 1A,B show voltammograms recorded before (dashed lines) and after (solid lines) 24 h. Initially, only background current flowed in each case, due to the poor electrocatalytic activity of GC for the HER. However, the HER onset potentials were −0.05 V and –0.1 V after 24 h using the Pt and Au counter electrodes, respectively. The HER overpotential at −10 mA cm^{-2} (which is commonly used as a measure of electrocatalytic performance) after 24 h electrolysis with a Pt counter electrode was

just 0.125 V more negative than when using a pure Pt electrocatalyst for the HER,[5] demonstrating the drastic activation of the GC that occurred over the test period.

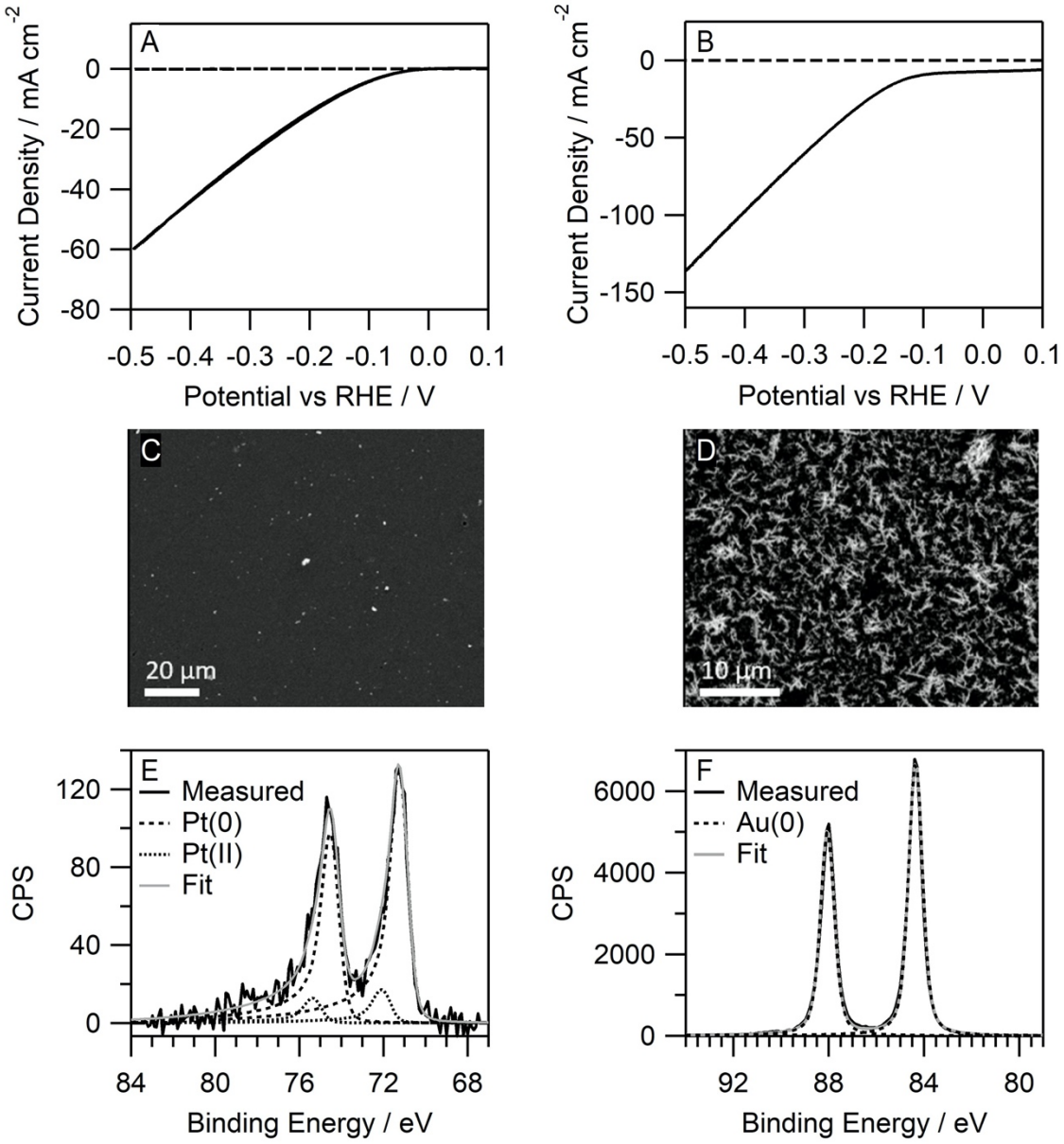

Figure 1. (A,B) Voltammograms recorded before and after 24 h of HER at GC at –10 mA cm^{-2} in a cell containing a Pt and Au counter electrode, respectively. (C,D) Scanning electron microscopy images of the GC surfaces after 24 h HER in a cell containing a Pt counter electrode and an Au counter electrode, respectively. (E,F) X-ray photoelectron spectra showing the presence of Pt and Au on the GC surface after the extended stability tests in which Pt and Au, respectively, were used as counter electrode.

SEM images of the GC surface after the stability test in which a Pt electrode was used (Figure 1C) revealed bright 700-1600 nm spots on the GC surfaces. The spots were identified as Pt islands using EDX analysis. Au dendrites were observed on the GC surface (Figure 1D) after the same experiment was carried out with an Au counter electrode. High-resolution XPS (Figures 1E,F) of the GC surfaces revealed doublets in the Pt and Au regions, which are attributable to the Pt $4f_{7/2}$, Pt $4f_{5/2}$, Au $4f_{7/2}$ and Au $4f_{5/2}$ signals, respectively. Deconvolution of the Pt peaks reveals that the Pt was 93% Pt(0) (71.3 and 74.6 eV)[32,37] and 7% Pt(II) (72.2 and 75.5 eV),[32,37] while the Au was predominantly Au(0).[38,39] Comparison of the areas of the Pt and Au peaks compared to those of C, O, N, and S yielded estimated Pt and Au surface concentrations of 0.21 and 10.0 at. %, respectively. The low quantity of Pt is similar to that observed by Zhang and co-workers, who deposited 0.08-0.16 monolayers of Pt onto a GC electrode during deliberate anodic dissolution of a Pt electrode and subsequent deposition of the dissolved Pt onto a carbon electrode for 2 h at −0.7 V *vs.* NHE.[40]

***Divided Cells for Mitigation of Metal Crossover*.** We repeated the extended stability tests by driving the HER at GC at −10 mA cm^{-2}, but this time we separated the GC from the counter and reference electrodes by a Nafion membrane. After 24 h using the Pt counter electrode, the concentration of Pt in the counter-electrode compartment was 31 ppb (measured by ICP-MS), while that in the HER compartment was 0.10 ppb. When a glass frit was used as the separator, the concentration of Pt in the HER compartment was 3.1 ppb, showing that the glass frit was more permeable to Pt ions. Figures 2A,B show XP spectra of the GC surfaces after 24 h of HER electrolysis with Pt and Au counter electrodes, revealing doublets similar to those in Figures 1E,F, and proving that the metals had deposited onto the GC surface, despite the presence of the Nafion barrier. Comparison of the dashed and solid black voltammograms of Figures 2C,D shows that the amounts of Pt and Au crossing the Nafion and depositing onto the GC were sufficient to decrease the onset potential for the HER to about –0.5 V and –0.4 V, respectively. The gray line of Figure 2C shows that use of the glass frit resulted in a larger decrease of the HER onset potential to about –0.2 V, due to the transport of more dissolved Pt across the frit. The HER overpotential at −10 mA cm^{-2} was −0.42 V and −0.67 V after using the glass frit and Nafion membrane, respectively, to separate the GC

from the Pt counter electrode. Use of the Nafion membrane to separate the Au counter electrode from the GC resulted in an HER overpotential at –10 mA cm^{-2} of –0.54 V after 24 h of electrolysis. These data prove that Nafion membranes, while more effective than glass frits, could not prevent contamination and activation of the GC surfaces by dissolved Pt and Au from counter electrodes during the HER.

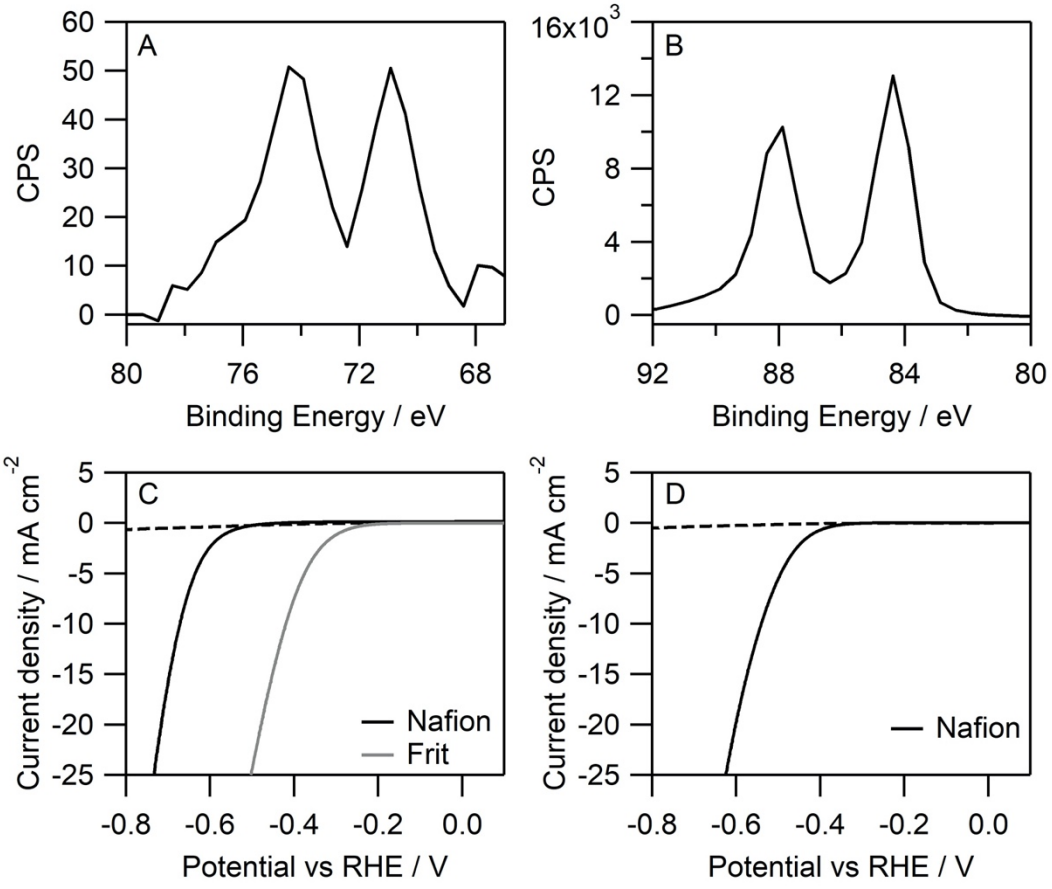

Figure 2. XP spectra of a GC surface after 24 h of HER at –10 mA cm^{-2} in cells containing (A) Pt and (B) Au counter electrodes, with a Nafion membrane separating the counter/reference electrodes from the GC. (C) Voltammograms recorded before (dashed line) and after (solid lines) 24 h of HER at –10 mA cm^{-2} at GC in cells containing a Pt counter electrodes and a Nafion-membrane (black solid line) and glass-frit separator (gray solid line), respectively. (D) Voltammograms recorded before (dashed line) and after (solid line) 24 h of HER at –10 mA cm^{-2} at GC in a cell containing an Au counter electrode and Nafion-membrane separator.

Figure 3A shows an SEM image of the GC electrode (HER) side of a membrane after 24 h electrolysis with an Au counter electrode. Bright spots are visible on the surface and the EDX map in Figure 3B confirms that these were Au particles. XPS analysis of the membrane (Figure 3C) revealed a doublet centred at 84.2 and 88 eV, corresponding to the $4f_{7/2}$ and $4f_{5/2}$ peaks of Au. SEM analysis of the membrane used with the Pt counter electrode revealed bright spots on both sides (Figures 4A,B), and EDX analysis confirmed they were Pt (Figure 4C). The presence of the metals on the Nafion can be attributed to reduction of metal ions crossing the membranes by H_2 generated at the GC surfaces over 24 h. A similar phenomenon has been observed during "post-mortem" analysis of Nafion membranes from proton-exchange membrane fuel cells.[41,42] Oxidation of Pt at fuel-cell cathodes releases mobile Pt^{2+}, which is reduced in the Nafion by H_2 supplied to the anode. That significantly less Pt than Au was detected on our membranes is presumably due to a lower concentration and/or slower reduction of dissolved Pt^{2+} ions in our systems. Indeed, XPS analysis of 3 random spots on the membrane surface failed to identify any Pt, due to its localization on the membrane surface (as evident from Figure 4A,B). The localised deposition of Pt may be due to microscopic inhomogeneities on the Nafion membrane acting as nucleation sites. Finally, and as a control experiment, we explored the transport of dissolved metals across the membrane in the absence of electrolysis. An H-cell containing 1.0 mol dm^{-3} H_2SO_4 on each side was constructed, and one side was spiked with 1 ppm Pt. A stirrer bar was used to emulate the rotation of the electrode on the non-spiked side. After 24 h, the non-spiked side contained 0.70 ppb Pt. The glass frit was nearly 8 times worse than the Nafion and allowed 5.5 ppb of Pt to build up in the non-spiked side of the cell.

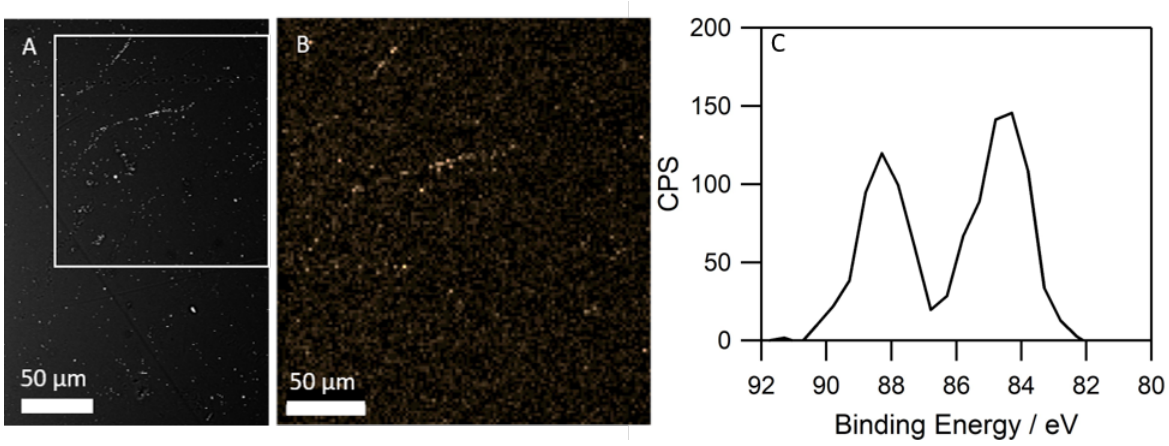

Figure 3. (A) Back-scattered electron SEM image of a Nafion membrane after 24 h of HER at –10 mA cm^{-2} at GC in a cell containing an Au counter electrode on the other side of the membrane. (B) EDX image of the boxed area in A, in which the orange spots correspond to Au. (C) High-resolution XP spectrum of the membrane surface in the Au region.

Use of Carbon Counter Electrodes to Mitigate against Metal Contamination. Given the problems associated with the use of metal counter electrodes, avoiding the use of metal seems a logical solution. It is generally thought that the use of graphite counter electrodes has no (or very little) influence on the activity of test electrocatalysts[8,22,24] and, consequently, this has been proposed as best practice for testing new materials.[3-5,7,8,11,24,35,36] However, as far as we can tell, no study has specifically reported on the use of graphite counter electrodes for extended constant-current HER tests, though some report the use of graphite counter electrodes for transient experiments.[8,24]

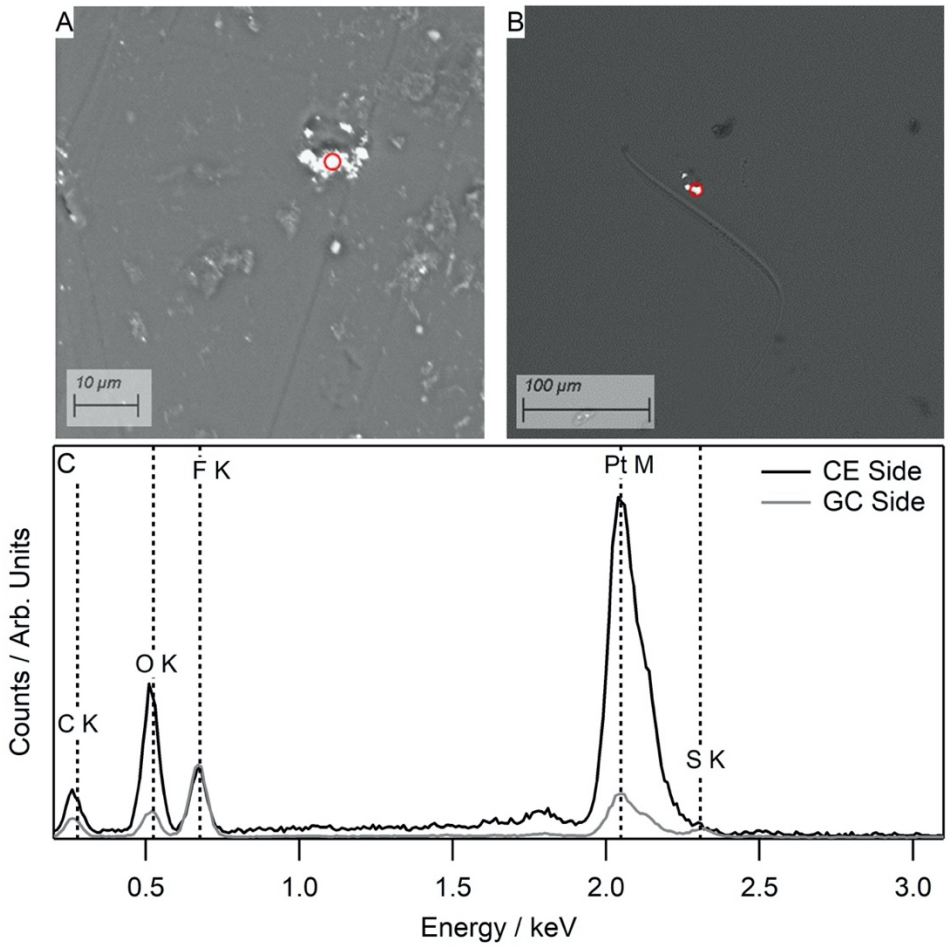

Figure 4. SEM images of Nafion after use in a divided cell containing a Pt counter electrode and in which the HER occurred for 24 h at GC at –10 mA cm^{-2}. (A) GC electrode (HER) side (B) counter-electrode (CE) side. (C) EDX spectra of both sides of the membrane. The red circles on the images show where EDX spectra were recorded. Spectra are normalized to the F K_α peak heights.

We first tested the effect of using of a graphite counter electrode in an undivided cell containing a polished Pt electrocatalyst for the HER. The black dashed line in Figure 5A shows the voltammogram recorded at the beginning of the test period. The HER onset potential was about 0.0 V, as expected for a Pt electrocatalyst. The solid black line shows the voltammogram recorded after 24 h. Remarkably, the magnitude of the HER overpotential at –10 mA cm^{-2} increased by more than 0.1 V over the test period, demonstrating that the electrocatalytic activity of the Pt surface decreased over the test period. Microscopic analysis of the surface of Pt after the stability test revealed that the surface had become

contaminated with carbonaceous spots (Figure 6). That we observe a large apparent decrease in the activity of Pt over 24 h of electrolysis using a carbon counter electrode, and such an effect has not been reported previously, may be a result of the HER occurring at a constant current density during the aging period, rather than by potential cycling.

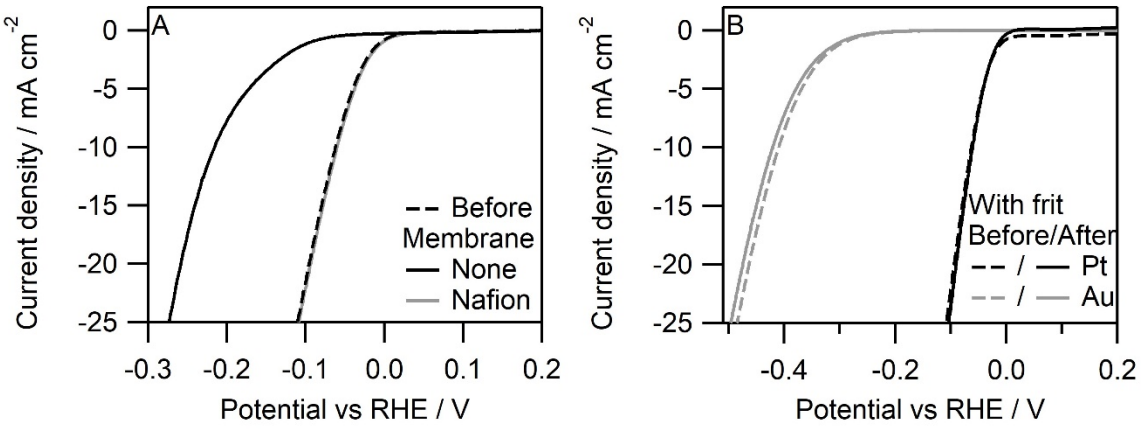

Figure 5. (A) Voltammograms recorded before (dashed line) and after (solid lines) 24 h of HER at –10 mA cm^{-2} at Pt in an undivided cell containing a graphite counter electrode. The gray line (which overlaps the black dashed line) shows the voltammogram recorded after the Pt electrocatalyst had been separated from the counter electrode by a Nafion membrane. (B) Voltammograms recorded before (dashed lines) and after (solid lines) 24 h of HER at –10 mA cm^{-2} in cells containing Pt (black) and Au (gray) electrocatalysts separated from a graphite counter electrode by a glass frit.

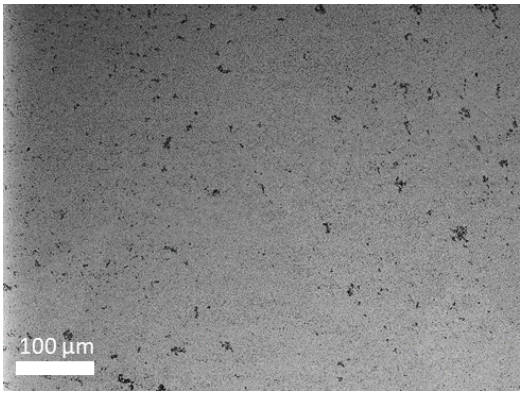

Figure 6. Back-scattered electron SEM image of a Pt surface after 24 h of HER at −10 mA cm^{-2} in an undivided cell containing a graphite counter electrode, showing contamination of the Pt with carbonaceous material (dark spots).

We then tested the effect of using a Nafion separator to isolate the carbon counter electrode from the Pt, and the resulting voltammogram is also presented in Figure 5A (gray solid line, which overlaps with the dashed line). No change in activity of the Pt electrode was observed during the test, indicating that the membrane had effectively prevented the crossover of contaminants from the graphite counter electrode. We also tested the effectiveness of using a glass frit to separate the carbon counter electrode from Pt and Au electrocatalysts, a common approach to electrocatalyst testing[5] (though to the best of our knowledge no published data has demonstrated the usefulness of this strategy). Figure 5B shows that after 24 h of HER, the voltammograms recorded using each electrocatalyst almost overlaid each other, demonstrating that the glass frit could effectively prevent deactivation of the electrocatalysts when graphite counter electrodes were used. We also investigated whether it was possible to use a GC rod instead of graphite as counter electrode in an undivided cell. In this case, a glass frit was also required to prevent contamination and deactivation of an Au electrocatalyst for the HER, a factor that could be attributed to flaking of the GC electrodes due to oxidation of graphitic domains.[43]

Electrocatalysis of H_2 Evolution at MoS_2 and $K_6[P_2W_{18}O_{62}](H_2O)_{14}$@SWNT. The implications of our observations were examined using MoS_2, which has been used as an earth-abundant HER electrocatalyst.[44,45] Testing and optimising such high-surface-area, earth-abundant electrocatalysts is of

significant interest to those interested in developing cost-effective materials for the H_2 generation. HER voltammograms were recorded using MoS_2 deposited onto a GC electrode before and after 24 h of constant-current HER using a Pt and graphite counter electrode (Figure 7). The graphite rod counter electrode was used with and without a glass frit separating it from the MoS_2. Before the extended stability test, the HER onset potential was about –0.25 V, which is typical of that expected for this electrocatalyst,[46] and the overpotential at −10 mA cm^{-2} was –0.437 V. The voltammogram recorded after 24 h of HER at –10 mA cm^{-2} in the undivided cell containing a Pt counter electrode (blue solid line) shows that a large decrease in the HER overpotential (at –10 mA cm^{-2}) to −0.144 V occurred during the test period. When a graphite rod was used in place of a Pt counter electrode, both with and without a glass frit separating it from the MoS_2 electrocatalyst, the voltammograms recorded before and after 24 h almost overlaid each other, and the overpotential at –10 mA cm^2 was similar in each case (dashed black line and gray and black solid lines). These observations demonstrate that the decrease in overpotential when using the Pt counter electrode was due to contamination of the MoS_2 with Pt, and that the use of the carbon electrode was necessary when studying the long-term stability of MoS_2. That the MoS_2 electrocatalyst was less susceptible to the effects of carbon contamination than the Pt and Au electrocatalysts may be due to the high availability of active sites in MoS_2. Moreover, deactivation of Pt by carbon is expected to be pronounced due to its high initial activity. Nonetheless, considering our data showing that carbon can be transported to the electrocatalyst surface during long-term polarization of HER electrocatalysts, we believe that it is prudent to use a glass frit to isolate the electrocatalyst surface from the carbon counter electrode.

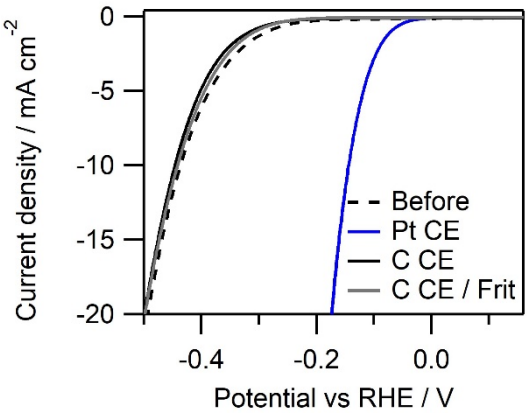

Figure 7. Voltammograms recorded before (dashed line) and after (solid lines) 24 h of HER at –10 mA cm^{-2} at a GC-electrode coated with MoS_2 in divided (black/grey solid lines) and undivided (blue solid line) cells containing a carbon or Pt counter electrode (CE).

Finally, we assessed whether our findings also applied to potential-cycling experiments. For this experiment, we chose a material comprising the Wells-Dawson tungsten polyoxometalate (POM) $K_6[P_2W_{18}O_{62}](H_2O)_{14}$ encapsulated within single-walled nanotubes ($K_6[P_2W_{18}O_{62}](H_2O)_{14}$@SWNT). This material has been described recently and represents a class of materials that offer unique opportunities for electrochemical applications.[47] A drop-cast film of this material on a GC electrode was cycled in Ar-purged 1.0 mol dm^{-3} HCl at 100 mV s^{-1}. The black voltammogram in Figure 8A shows 3 sets of redox waves in the potential region between −0.1 and −0.7 V, attributable to the following redox couples (from most positive to most negative):

$$[P_2W_{18}O_{62}]^{6-} + 2e^- \leftrightarrow [P_2W_{18}O_{62}]^{8-} \quad (1)$$

$$[P_2W_{18}O_{62}]^{6-} + 2e^- + 2H^+ \leftrightarrow [H_2P_2W_{18}O_{62}]^{8-} \quad (2)$$

$$[H_2P_2W_{18}O_{62}]^{8-} + 2e^- + 2H^+ \leftrightarrow [H_4P_2W_{18}O_{62}]^{8-} \quad (3)$$

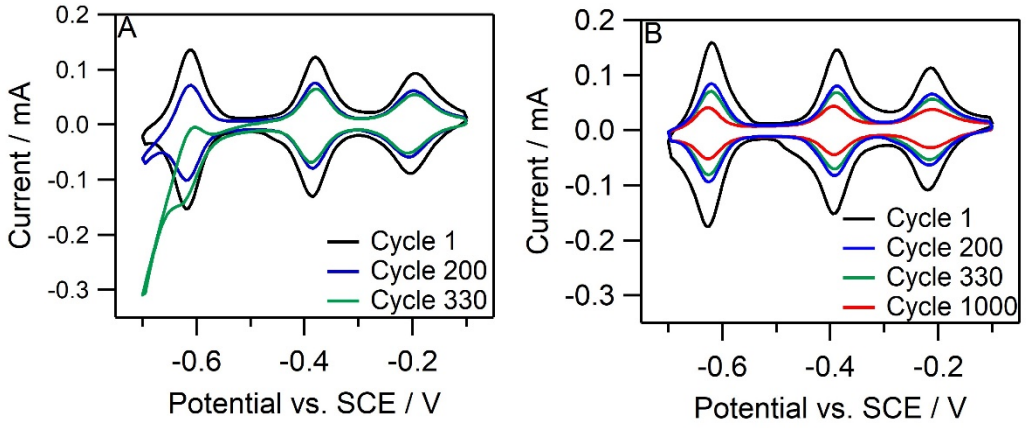

Figure 8. The 1st, 200th, and 330th cyclic voltammograms of $K_6[P_2W_{18}O_{62}](H_2O)_{14}$@SWNT deposited onto a stationary GC electrode and cycled at 100 mV s^{-1} in an undivided cell containing (A) a Pt counter electrode and (B) a GC-rod counter electrode.

The bell shape of the voltammetric peaks in Figure 8 can be attributed to confinement of the composite on the electrode surface (that is, the peaks show non-diffusional responses). After fewer than 200 electrochemical cycles in an undivided cell containing a Pt counter electrode (Figure 8A), the peak currents decreased due to slow loss of the material from the electrode. However, by the 300th cycle, a large increase in cathodic current appeared at potentials negative of about –0.6 V. This effect has been observed previously during solution-phase electrochemistry of POMs and was originally attributed to the formation of a POM-derived HER electrocatalyst upon potential cycling.[48,49] It has since been shown that this increase in electrocatalytic HER activity was due to migration of dissolved Pt from Pt counter electrodes onto the electrode surface, which catalyzed the HER.[26] Zhang et al. have used this phenomenon to produce highly active silicotungstate POM electrocatalysts.[40]

We repeated the cycling experiments using our $K_6[P_2W_{18}O_{62}](H_2O)_{14}$@SWNT composite electrode and a GC counter electrode instead of a Pt counter electrode (Figure 8B), and found that the HER current at potentials negative of −0.6 V no longer appeared. The only change in the voltammograms was the decrease in the peak areas, due to loss of the active POMs from the electrode. Furthermore, we found

that after 330 cycles in the cell containing the Pt counter electrode, there was significant H_2 bubble formation on the electrode surface due to the HER, preventing meaningful voltammograms from being recorded. In contrast, when a GC counter electrode was used no bubble formed at the electrode surface, further demonstrating that the use of a carbon electrode in this system was necessary to avoid the problems associated with the use of Pt counter electrodes.

CONCLUSIONS

H_2 evolution in cells containing Pt and Au counter electrodes leads to dissolution of the counter electrodes and results in metal deposition onto glassy-carbon electrocatalysts in undivided electrochemical cells, increasing the electrocatalytic activity of the carbon surface for H_2 evolution. Nafion membranes cannot prevent this contamination of the electrode. The use of graphite and glassy carbon counter electrodes can cause the opposite problem, contaminating Pt and Au electrocatalysts and decreasing their activities significantly. This phenomenon can be avoided by using a carbon counter electrode separated from the electrocatalyst by a glass frit. The effects of using noble-metal counter electrodes and separators to isolate test electrocatalysts was demonstrated using a MoS_2 electrocatalyst for H_2 evolution. We also showed that potential-cycling of polyoxometalate-based composite electrodes is sensitive to contamination by Pt from counter electrodes, but this can be prevented using a carbon counter electrode. We recommend that divided cells containing carbon-based counter electrodes are used when analysing the performance of electrocatalysts for H_2 evolution, to avoid the reporting of erroneously high or low performance metrics for electrocatalysts for H_2 evolution. This approach will save time and resources as we face the important challenge of finding new materials for the emerging hydrogen economy.

AUTHOR CONTRIBUTIONS

The manuscript was written by all authors. All authors have given approval to the final version of the manuscript.

NOTES

The authors declare no competing financial interest

ACKNOWLEDGMENTS

We thank the EPSRC for funding through Projects EP/L015749/1 and EP/P002382/1, the University of Nottingham for funding through the Beacon of Excellence in Propulsion Futures. We thank Dr. Emily Smith and Dr. Craig Stoppiello at the Nanoscale and Microscale Research Centre at the University of Nottingham for recording and assisting with XPS, and Dr. Scott Young and Saul Vazquez Reina in the School of Biosciences at the University of Nottingham for recording and assisting with ICP-MS. We thank Beth Mortiboy for help with voltammetry.

REFERENCES

(1) Shao, M.; Chang, Q.; Dodelet, J. P.; Chenitz, R., Recent Advances in Electrocatalysts for Oxygen Reduction Reaction. *Chem. Rev.* **2016**, *116*, 3594-3657.

(2) Garsany, Y.; Baturina, O. A.; Swider-Lyons, K. E.; Kocha, S. S., Experimental Methods for Quantifying the Activity of Platinum Electrocatalysts for the Oxygen Reduction Reaction. *Anal. Chem.* **2010**, *82*, 6321-6328.

(3) Voiry, D.; Chhowalla, M.; Gogotsi, Y.; Kotov, N. A.; Li, Y.; Penner, R. M.; Schaak, R. E.; Weiss, P. S., Best Practices for Reporting Electrocatalytic Performance of Nanomaterials. *ACS Nano* **2018**, *12*, 9635-9638.

(4) McCrory, C. C.; Jung, S.; Peters, J. C.; Jaramillo, T. F., Benchmarking Heterogeneous Electrocatalysts for the Oxygen Evolution Reaction. *J. Am. Chem. Soc.* **2013**, *135*, 16977-16987.

(5) McCrory, C. C.; Jung, S.; Ferrer, I. M.; Chatman, S. M.; Peters, J. C.; Jaramillo, T. F., Benchmarking Hydrogen Evolving Reaction and Oxygen Evolving Reaction Electrocatalysts for Solar Water Splitting Devices. *J. Am. Chem. Soc.* **2015**, *137*, 4347-4357.

(6) Benck, J. D.; Pinaud, B. A.; Gorlin, Y.; Jaramillo, T. F., Substrate Selection for Fundamental Studies of Electrocatalysts and Photoelectrodes: Inert Potential Windows in Acidic, Neutral, and Basic Electrolyte. *PLoS One* **2014,** *9*, e107942.

(7) Chen, J. G.; Jones, C. W.; Linic, S.; Stamenkovic, V. R., Best Practices in Pursuit of Topics in Heterogeneous Electrocatalysis. *ACS Catal*. **2017,** *7*, 6392-6393.

(8) Li, J.; Liu, H. Y.; Lu, Y.; Guo, X. W.; Song, Y. J., Influence of Counter Electrode Material during Accelerated Durability Test of Non-precious Metal Electrocatalysts in Acidic Medium. *Chin. J. Catal*. **2016,** *37* (7), 1109-1118.

(9) Hong, W. T.; Risch, M.; Stoerzinger, K. A.; Grimaud, A.; Suntivich, J.; Shao-Horn, Y., Toward the Rational Design of Non-precious Transition Metal Oxides for Oxygen Electrocatalysis. *Energy Environ. Sci*. **2015**, *8*, 1404-1427.

(10) Dekanski, A.; Stevanovic, J.; Stevanovic, R.; Nikolic, B. Z.; Jovanovic, V. M., Glassy Carbon Electrodes I. Characterization and Electrochemical Activation. *Carbon* **2001**, *39*, 1195-1205.

(11) Bystron, T.; Sramkova, E.; Dvorak, F.; Bouzek, K., Glassy Carbon Electrode Activation - A Way towards Highly Active, Reproducible and Stable Electrode Surface. *Electrochim. Acta* **2019**, *299*, 963-970.

(12) Chen, R.; Yang, C. J.; Cai, W. Z.; Wang, H. Y.; Miao, J. W.; Zhang, L. P.; Chen, S. L.; Liu, B., Use of Platinum as the Counter Electrode to Study the Activity of Nonprecious Metal Catalysts for the Hydrogen Evolution Reaction. *ACS Energy Lett*. **2017**, *2*, 1070-1075.

(13) Elgrishi, N.; Rountree, K. J.; McCarthy, B. D.; Rountree, E. S.; Eisenhart, T. T.; Dempsey, J. L., A Practical Beginner's Guide to Cyclic Voltammetry. *J. Chem. Ed*. **2018**, *95*, 197-206.

(14) Cherevko, S.; Zeradjanin, A. R.; Keeley, G. P.; Mayrhofer, K. J. J., A Comparative Study on Gold and Platinum Dissolution in Acidic and Alkaline Media. *J. Electrochem. Soc*. **2014**, *161*, H822-H830.

(15) Fei, H.; Dong, J.; Arellano-Jiménez, M. J.; Ye, G.; Dong Kim, N.; Samuel, E. L. G.; Peng, Z.; Zhu, Z.; Qin, F.; Bao, J.; Yacaman, M. J.; Ajayan, P. M.; Chen, D.; Tour, J. M., Atomic Cobalt on Nitrogen-doped Graphene for Hydrogen Generation. *Nature Commun*. **2015**, *6*, 8668.

(16) Arulmozhi, N.; Esau, D.; Lamsal, R. P.; Beauchemin, D.; Jerkiewicz, G., Structural Transformation of Monocrystalline Platinum Electrodes upon Electro-oxidation and Electro-dissolution. *ACS Catal*. **2018**, *8*, 6426-6439.

(17) Cherevko, S.; Kulyk, N.; Mayrhofer, K. J. J., Durability of Platinum-based Fuel Cell Electrocatalysts: Dissolution of Bulk and Nanoscale Platinum. *Nano Energy* **2016**, *29*, 275-298.

(18) Topalov, A. A.; Katsounaros, I.; Auinger, M.; Cherevko, S.; Meier, J. C.; Klemm, S. O.; Mayrhofer, K. J., Dissolution of Platinum: Limits for the Deployment of Electrochemical Energy Conversion? *Angew. Chem. Int. Ed*. **2012**, *51*, 12613-12615.

(19) Topalov, A. A.; Cherevko, S.; Zeradjanin, A. R.; Meier, J. C.; Katsounaros, I.; Mayrhofer, K. J. J., Towards a Comprehensive Understanding of Platinum Dissolution in Acidic Media. *Chem. Sci*. **2014**, *5*, 631-638.

(20) Matsumoto, M.; Miyazaki, T.; Imai, H., Oxygen-Enhanced Dissolution of Platinum in Acidic Electrochemical Environments. *J. Phys. Chem. C* **2011**, *115*, 11163-11169.

(21) Inoue, M.; Nakazawa, A.; Umeda, M., Study of Pt Electrode Dissolution in H_2O_2-containing H_2SO_4 Solution using an Electrochemical Quartz Crystal Microbalance. *J. Power Sources* **2011**, *196*, 4579-4582.

(22) Wei, R.; Fang, M.; Dong, G.; Ho, J. C., Is Platinum a Suitable Counter Electrode Material for Electrochemical Hydrogen Evolution Reaction? *Science Bull*. **2017**, *62*, 971-973.

(23) Xing, L. Y.; Hossain, M.; Tian, M.; Beauchemin, D.; Adjemian, K.; Jerkiewicz, G., Platinum Electro-dissolution in Acidic Media upon Potential Cycling. *Electrocatalysis* **2014**, *5*, 96-112.

(24) Dong, G. F.; Fang, M.; Wang, H. T.; Yip, S.; Cheung, H. Y.; Wang, F. Y.; Wong, C. Y.; Chu, S. T.; Ho, J. C., Insight into the Electrochemical Activation of Carbon-based Cathodes for Hydrogen Evolution Reaction. *J. Mater. Chem. A* **2015**, *3*, 13080-13086.

(25) Xu, X. X.; Makaraviciute, A.; Pettersson, J.; Zhang, S. L.; Nyholm, L.; Zhang, Z., Revisiting the Factors influencing Gold Electrodes prepared using Cyclic Voltammetry. *Sens. Actuators B Chem.* **2019**, *283*, 146-153.

(26) Kulesza, P. J.; Lu, W. Y.; Faulkner, L. R., Cathodic Fabrication of Platinum Microparticles via Anodic Dissolution of a Platinum Counter Electrode – Electrocatalytic Probing and Surface-analysis of Dispersed Platinum. *J. Electroanal. Chem.* **1992**, *336*, 35-44.

(27) Tian, M.; Cousins, C.; Beauchemin, D.; Furuya, Y.; Ohma, A.; Jerkiewicz, G., Influence of the Working and Counter Electrode Surface Area Ratios on the Dissolution of Platinum under Electrochemical Conditions. *ACS Catal.* **2016**, *6*, 5108-5116.

(28) Popczun, E. J.; McKone, J. R.; Read, C. G.; Biacchi, A. J.; Wiltrout, A. M.; Lewis, N. S.; Schaak, R. E., Nanostructured Nickel Phosphide as an Electrocatalyst for the Hydrogen Evolution Reaction. *J. Am. Chem. Soc.* **2013**, *135*, 9267-9270.

(29) Roy, C.; Rao, R. R.; Stoerzinger, K. A.; Hwang, J.; Rossmeisl, J.; Chorkendorff, I.; Shao-Horn, Y.; Stephens, I. E. L., Trends in Activity and Dissolution on RuO_2 under Oxygen Evolution Conditions: Particles versus Well-Defined Extended Surfaces. *ACS Energy Lett.* **2018**, *3*, 2045-2051.

(30) Burlatsky, S. F.; Gummalla, M.; Atrazhev, V. V.; Dmitriev, D. V.; Kuzminyh, N. Y.; Erikhman, N. S., The Dynamics of Platinum Precipitation in an Ion Exchange Membrane. *J. Electrochem. Soc.* **2011**, *158*, B322-B330.

(31) Yasuda, K.; Taniguchi, A.; Akita, T.; Ioroi, T.; Siroma, Z., Platinum Dissolution and Deposition in the Polymer Electrolyte Membrane of a PEM Fuel Cell as studied by Potential Cycling. *Phys. Chem. Chem. Phys.* **2006**, *8*, 746-752.

(32) Peron, J.; Nedellec, Y.; Jones, D.; Roziere, J., The Effect of Dissolution, Migration and Precipitation of Platinum in Nafion-based Membrane Electrode Assemblies during Fuel Cell Operation at High Potential. *J. Power Sources* **2008**, *185*, 1209-1217.

(33) Ohma, A.; Suga, S.; Yamamoto, S.; Shinohara, K., Membrane Degradation Behavior during Open-circuit Voltage Hold Test. *J. Electrochem. Soc.* **2007**, *154*, B757-B760.

(34) Hawut, W.; Hunsom, M.; Pruksathorn, K., Platinum Electroless Deposition on Nafion Membrane for PEM Fuel Cells. *Korean J. Chem. Eng.* **2006**, *23*, 555-559.

(35) Wu, G.; More, K. L.; Johnston, C. M.; Zelenay, P., High-performance Electrocatalysts for Oxygen Reduction derived from Polyaniline, Iron, and Cobalt. *Science* **2011**, *332*, 443-447.

(36) Lin, C.; Gao, Z. F.; Yang, J. H.; Liu, B.; Jin, J., Porous Superstructures Constructed from Ultrafine FeP Nanoparticles for Highly Active and Exceptionally Stable Hydrogen Evolution Reaction. *J. Mater. Chem. A* **2018**, *6*, 6387-6392.

(37) Hammond, J. S.; Winograd, N., XPS Spectroscopic Study of Potentiostatic and Galvanostatic Oxidation of Pt Electrodes in H_2SO_4 and $HClO_4$. *J. Electroanal. Chem.* **1977**, *78*, 55-69.

(38) Casaletto, M. P.; Longo, A.; Martorana, A.; Prestianni, A.; Venezia, A. M., XPS Study of Supported Gold Catalysts: The Role of Au(0) and $Au^{+\delta}$ Species as Active Sites. *Surf. Interface Anal.* **2006**, *38*, 215-218.

(39) Schneider, W. D.; Laubschat, C., Actinide-Noble-Metal Systems - an X-Ray-Photoelectron-Spectroscopy Study of Thorium-Platinum, Uranium-Platinum, and Uranium-Gold Intermetallics. *Phys. Rev. B* **1981**, *23*, 997-1005.

(40) Zhang, C.; Hong, Y.; Dai, R.; Lin, X.; Long, L.-S.; Wang, C.; Lin, W., Highly Active Hydrogen Evolution Electrodes via Co-Deposition of Platinum and Polyoxometalates. *ACS Appl. Mater. Interfaces* **2015**, *7*, 11648-11653.

(41) Zaton, M.; Roziere, J.; Jones, D. J., Current Understanding of Chemical Degradation Mechanisms of Perfluorosulfonic Acid Membranes and their Mitigation Strategies: A Review. *Sust. Energy Fuel.* **2017**, *1*, 409-438.

(42) Macauley, N.; Wong, K. H.; Watson, M.; Kjeang, E., Favorable Effect of In-situ Generated Platinum in the Membrane on Fuel Cell Membrane Durability. *J. Power Sources* **2015**, *299*, 139-148.

(43) Yi, Y.; Weinberg, G.; Prenzel, M.; Greiner, M.; Heumann, S.; Becker, S.; Schlögl, R., Electrochemical Corrosion of a Glassy Carbon Electrode. *Catal. Today* **2017**, *295*, 32-40.

(44) Zhuang, Z.; Huang, J.; Li, Y.; Zhou, L.; Mai, L., The Holy Grail in Platinum-Free Electrocatalytic Hydrogen Evolution: Molybdenum-Based Catalysts and Recent Advances. *ChemElectroChem* **2019**, *6*, 3570-3589.

(45) Benck, J. D.; Chen, Z.; Kuritzky, L. Y.; Forman, A. J.; Jaramillo, T. F., Amorphous Molybdenum Sulfide Catalysts for Electrochemical Hydrogen Production: Insights into the Origin of their Catalytic Activity. *ACS Catal*. **2012**, *2*, 1916-1923.

(46) Yu, Y; Huang, S. -Y; Li, Y; Steinmann, S. N.; Yang, W.; Cao, L., Layer-Dependent Electrocatalysis of MoS_2 for Hydrogen Evolution, *Nano Lett*. **2014**, *14*, 553-558.

(47) Jordan, J. W; Lowe, G. L.; McSweeney, R. L.; Stoppiello, C. T.; Lodge, R. W; Skowron, S. T.; Biskupek, J.; Rance, G. A.; Kaiser, U.; Walsh, D. A; Newton, G. N.; Khlobystov, A. N., Host–Guest Hybrid Redox Materials Self-Assembled from Polyoxometalates and Single-Walled Carbon Nanotubes. *Adv. Mater.* **2019**, *31*, 1904182.

(48) Keita, B.; Nadjo, L., Activation of Electrode Surfaces: Application to the Electrocatalysis of the Hydrogen Evolution Reaction. *J. Electroanal. Chem*. **1985**, *191*, 441-448.

(49) Keita, B.; Nadjo, L., New Oxometalate-based Materials for Catalysis and Electrocatalysis. *Mater. Chem. Phys*. **1989**, *22*, 77-103.

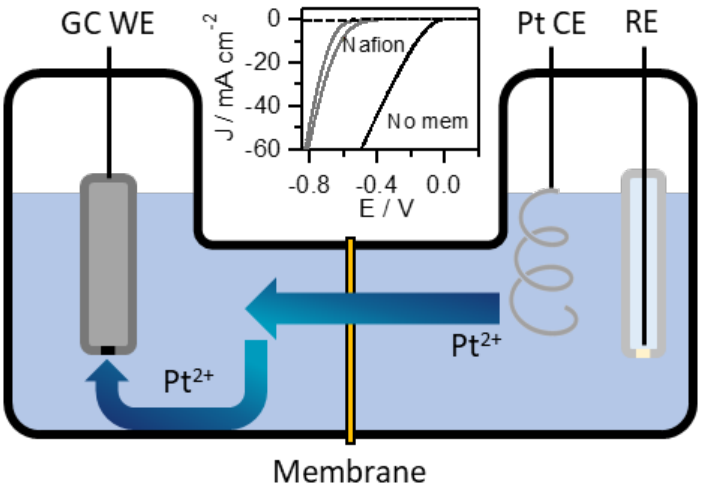

ToC artwork